IRAQI Academic Scientific Journals

SAMARRA JOURNAL OF ENGINEERING SCIENCE AND RESEARCH

S.J.E.S.R

# Simulation of Heat Exchanger Dynamics and Its Control Study by Using MATLAB

**Zainab Abdulmaged Khalaf [1*], Maria Rasheed Jassim [2] , Firas Qassim Mohammed [3] and Taghred Flayyih Hasan [4]**

**1- Department of Electromechanical Engineering, College of Engineering, University of Samarra, Iraq**
**2- Department of Electromechanical Engineering, College of Engineering, University of Samarra, Iraq**
**3- Department of Electromechanical Engineering, College of Engineering, University of Samarra, Iraq**
**4- Department of Architectural Engineering, College of Engineering, University of Samarra, Iraq**

**Article Information**
**Received: 16/12/2023**
**Accepted: 04/01/2024**
**Keywords:**
***Heat Exchanger, Modelling, PID, MATLAB***

**Corresponding Author**
**E-mail:**
*Zainab.abd@uosamarra.edu.iq*
**Mobile:**
**07708357683**

**Abstract**

The most popular heat exchanger is one that transfers heat between two fluids from one region with a high temperature to another one with a lower temperature when compared to the first one for achieving thermal equilibrium. It can be utilized for heating or cooling. MATLAB is used to build the heat exchanger's simulation, which is the shell and tube heat exchanger process, to examine how the process responds under various operating situations. The system's mathematical model was then derived to implement the control system. To determine the optimal sort of control system, various types of control systems have been used. By comparing the PID type control system to other control systems about both settling time and bypass or percentage overshoot, the results showed that it is the best control system.

## Introduction:

A tube bundle enclosed in a cylindrical shell is essentially what makes up a shell and tube exchanger. The fluids on the shell and tube sides are separated by the tube sheets into which the tubes' ends are put [1]. In order to control the fluid flow and support the tubes, the shell incorporates baffles. In contrast to the previous study, Zhang et al. in 2009 simulated heat transfer in shell and tube heat exchangers using a different model that utilized helical baffles, and they discovered that the heat transfer coefficient is rising [2]. The simulation's main goal is to allow you to make changes to the mathematical model and see how they will affect the system without having to actually implement them until being certain that they will both improve the device's performance and lessen the problems that would otherwise have to be dealt with in real life. We are unsure if it will increase the device's performance because of its price of reality changing. PID control is used to simulate heat transfer control for a shell-and-tube heat exchanger system. They created a shell-and-tube heat exchanger mathematical model and transformed it into a PID system. System stability is necessary, and they looked at several ways to regulate the exit fluid's temperature, noting that the internal model-based PID controller performs satisfactorily in both transient state and steady state [3]. When put to comparison with the conventional controller, the PID controller created using the in-house model demonstrated a 44.6% improvement in time stability and 84% improvement in

overtaking [4]. Many researchers created MATLAB simulation for controlling the temperature of the fluid leaving the heat exchanger. They utilized a different mathematical model from their earlier research, in which they utilized many types of controllers to determine which had the best and quickest response times [5,6].

Heat exchangers are one of the most basic and crucial components utilized in various industrial operations and processes, with Shell and Tube heat exchanger systems being the most utilised because it can withstand a broad range of pressure and temperature values [7-9]. The primary goal is to keep precise control over the exit temperature of the various operating conditions. An internal model control strategy is used in conjunction with the disturbance rejection function in this [10]. The temperature of Shell's outlet fluid is regulated using a PID (Proportional – Integral – Derivative) controller in conjunction with feed-forward controllers to counteract disturbance fluid flow [11]. Modelling and control of a real-time shell and tube heat exchanger was published in 2017 by Sahoo. They demonstrate through the results of their experiments that the IMC-based PID controller causes the system to reach the necessary set point earlier than the auto-tuned PID controller for the relay. It is clear from both regulatory responses that the IMC-based PID controller, as opposed to the auto-tuned PID controller, causes the system to respond to perturbations earlier and return to the set point more quickly than the prior status [12].

**Mathematical Modelling and Simulation:**

The mathematical modelling of shell and tube heat exchanger, simulation study and control:

• Mathematical models were derived based on energy balances.

• MATLAB was utilized for simulating the dynamic system and study the response of the system

• The PID controller was used to control the temperature and the response regarding the system for reaching the steady state and the other controller.

The modelling assumptions are:

1. Constant specific heat (which is, pressure and temperature independent).
2. Adiabatic conditions (no exchange of heat with environment).
3. Constant mass flow rates for the two fluids across heat exchanger tubes.
4. Constant overall heat transfer coefficient U across heat exchanger.
5. Negligible axial conduction along tubes.

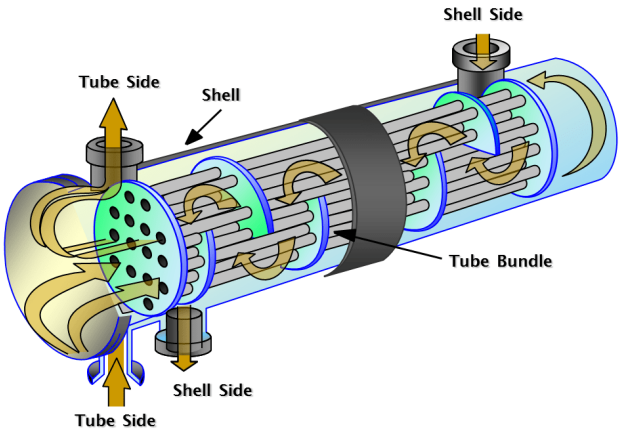


**Fig. 1** *The diagram of shell and tube heat exchanger.*

The amount of heat that enters the tube side relies on the flow rate and temperature of cold water:

$$q_{c_o} = \dot{m}_c c_{p_c}\left(T_{c_i} - T_{c_o}\right) + q_{c_{in}} \qquad (1)$$

**Where;**

$q_c$ ... heat energy flow for tube side in J/sec

$\dot{m}_c$ ... mass flow rate of the tube side in kg/sec

$c_{p_c}$ ... heat capacity of the tube side in J/kg. ℃

$q_{cin}$ ... the heat energy addition to tube side from surrounding in J/sec

$T_{c_i}, T_{c_o}$ ... inlet and outlet temperature of the tube side in ℃

$c_{p_c}$ ... heat capacity of the tube side in J/kg. ℃

to find the $q_{c_o}$ and $q_{c_{in}}$

$$q_{c_o} = \dot{m}_c c_{p_c} T_{c_o}$$

$$m = \rho . V$$

$$\frac{dq_{c_o}}{dt} = \rho_c V_c c_{p_c} \frac{dT_{c_o}}{dt}$$

Where;

$\rho_c$ ... density of the cold liquid in $kg/m^3$

$V_c$ ... volume of the tube side $m^3$

By taking the integration for this equation.

$$q_{c_o} = \rho_c V_c c_{p_c} T_{c_o}(t) \qquad (2)$$

$$dq_{c_{in}} = U_c A_c \frac{d}{dt}(T_{h_o} - T_{c_o})$$

$$\therefore q_{c_{in}} = U_c A_c \left(T_{h_o}(t) - T_{c_o}(t)\right) \qquad (3)$$

By substituting eq. (2) and eq. (3) into eq. (1) we get.

$$T_{c_o}(t) = \frac{\dot{m}_c}{\rho_c V_c}\left(T_{c_{in}}(t) - T_{c_o}(t)\right) + \frac{U_c A_c}{\rho_c V_c c_{p_c}}\left(T_{h_o}(t) - T_{c_o}(t)\right)$$

The hot-water flow rate and temperature affect how much heat enters the tube side:

$$q_{h_o} = \dot{m}_h c_{p_h}\left(T_{h_i} - T_{h_o}\right) + q_{h_{in}} \qquad (4)$$

Where;

$q_h$ ... heat energy flow for shell side in J/sec

$\dot{m}_h$ ... mass flow rate of the shell side in kg/sec

$c_{p_h}$ ... heat capacity of the shell side in J/kg. ℃

$q_{hin}$ ... the heat energy addition to shell side from surrounding in J/sec

$T_{h_i}, T_{h_o}$ ... inlet and outlet temperature of the shell side in ℃

$c_{p_h}$ ... heat capacity of the shell side in J/kg. ℃

To find the $q_{h_o}$ and $q_{h_{in}}$

$$q_{h_o} = \dot{m}_h c_{p_h} T_{h_o}$$

$$\frac{dq_{h_o}}{dt} = \rho_h V_h c_{p_h} \frac{dT_{h_o}}{dt}$$

Where;

$\rho_h$ ... density of the hot liquid in $kg/m^3$

$V_h$ ... volume of the shell side $m^3$

By taking the integration for this equation.

$$q_{h_o} = \rho_h V_h c_{p_h} T_{h_o}(t) \qquad (5)$$

$$dq_{h_{in}} = U_h A_h \frac{d}{dt}(T_{c_o} - T_{h_o})$$

$$\therefore q_{h_{in}} = U_h A_h \left(T_{c_o}(t) - T_{h_o}(t)\right) \qquad (6)$$

By substituting eq. (5) and eq. (6) into eq. (4) we can get.

$$T_{h_o}(t) = \frac{\dot{m}_h}{\rho_h V_h}\left(T_{h_{in}}(t) - T_{h_o}(t)\right) + \frac{U_h A_h}{\rho_h V_h c_{p_h}}\left(T_{c_o}(t) - T_{h_o}(t)\right)$$

*Transfer function of tube side*

$$q_{c_o} = m_c c_{P_c}\left(T_{c_{in}} - T_{c_o}\right) + q_{c_{in}} \qquad (7)$$

$$q_{c_{in}} = U_c A_c\left(T_{h_o} - T_{c_o}\right) \qquad (8)$$

$$q_{c_o} = \rho_c V_c c_{P_c} T_{c_o} \Longrightarrow \frac{dq_{c_o}}{dt} = \rho_c V_c c_{P_c} \frac{dT_{c_o}}{dt} \qquad (9)$$

Sub eq. (8) & (9) in eq. (7):-

$$\rho_c V_c c_{P_c} \frac{dT_{c_o}(t)}{dt} = m_c c_{P_c}\left(T_{c_{in}}(t) - T_{c_o}(t)\right) + U_c A_c\left(T_{h_o}(t) - T_{c_o}(t)\right)$$

$$\tau_1 = \frac{\rho_c V_c c_{P_c}}{m_c c_{P_c} + U_c A_c}$$

$$K_1 = \frac{m_c c_{P_c}}{m_c c_{P_c} + U_c A_c}$$

$$K_2 = \frac{U_c A_c}{m_c c_{P_c} + U_c A_c}$$

$$\tau_1 \frac{dT_{c_o}(t)}{dt} + T_{c_o}(t) = K_1 T_{c_{in}}(t) + K_2 T_{h_o}(t) \qquad (10)$$

The Laplace transform of the function of time f(t) which is written as $\mathcal{L}\{f_{(t)}\}$, is this [4]:

$$\mathcal{L}\{f_{(t)}\} = \int_0^\infty e^{-st} f(t)\, dt \qquad (11)$$

F(s) denotes a function of the form (s). It is customary to write the Laplace transform with a capital F and the time-varying function f(t) with a lowercase f, as in the following:

$$\mathcal{L}\{f_{(t)}\} = F(s) \qquad (12)$$

Laplace transform of a function derivative is given by:

$$\mathcal{L}\left\{\frac{d}{dt} f_{(t)}\right\} = S\,F(s) - f(0) \qquad (13)$$

Where $f(0)$ is the value of the function when $t = 0$.

By taking L.T. for eq. (10) and make $T_{c_{in}}$ in initial condition

$$\tau_1 s T_{c_o}(s) + T_{c_o}(s) = K_1 T_{c_{in}}(s) + K_2 T_{h_o}(s)$$

$$(\tau_1 s + 1) T_{c_o}(s) = K_2 T_{h_o}(s)$$

$$G_1(s) = \frac{T_{c_o}(s)}{T_{h_o}(s)} = \frac{K_2}{\tau_1 s + 1} \qquad (14)$$

*Transfer function of Shell side*

$$q_{h_o} = m_h c_{P_h}\left(T_{h_{in}} - T_{h_o}\right) + q_{h_{in}} \qquad (15)$$

$$q_{h_{in}} = U_h A_h\left(T_{c_o} - T_{h_o}\right) \qquad (16)$$

$$q_{h_o} = \rho_h V_h c_{P_h} T_{h_o} \Longrightarrow \frac{dq_{h_o}}{dt} = \rho_h V_h c_{P_h} \frac{dT_{h_o}}{dt} \qquad (17)$$

Sub eq. (16) & (17) in eq. (15):-

$$\rho_h V_h c_{P_h} \frac{dT_{h_o}(t)}{dt} = m_h c_{P_h}\left(T_{h_{in}}(t) - T_{h_o}(t)\right) + U_h A_h\left(T_{c_o}(t) - T_{h_o}(t)\right)$$

$$\frac{\rho_h V_h c_{P_h}}{m_h c_{P_h} + U_h A_h}\frac{dT_{h_o}(t)}{dt} + T_{h_o}(t) = \frac{m_h c_{P_h}}{m_h c_{P_h} + U_h A_h}T_{h_{in}}(t) + \frac{U_h A_h}{m_h c_{P_h} + U_h A_h}T_{c_o}(t)$$

$$\tau_2 = \frac{\rho_h V_h c_{P_h}}{m_h c_{P_h} + U_h A_h}$$

$$K_3 = \frac{m_h c_{P_h}}{m_h c_{P_h} + U_h A_h}$$

$$K_4 = \frac{U_h A_h}{m_h c_{P_h} + U_h A_h}$$

$$\tau_2 \frac{dT_{h_o}(t)}{dt} + T_{h_o}(t) = K_3 T_{h_{in}}(t) + K_4 T_{c_o}(t) \qquad (18)$$

Taking Laplace transform for eq. (9)

$$\tau_2 s T_{h_o}(s) + T_{h_o}(s) = K_3 T_{h_{in}}(s) + K_4 T_{c_o}(s) \qquad (19)$$

$$(\tau_2 s + 1)T_{h_o}(s) = K_4 T_{c_o}(s)$$

$$G_2(s) = \frac{T_{h_o}(s)}{T_{c_o}(s)} = \frac{K_4}{\tau_2 s + 1} \qquad (20)$$

The control valve has a maximum steam capacity of 2.1 kg per second, linear properties, and a 3 second time constant. The valve's nominal pressure range is between 3 and 15 psig.

$$\text{Valve gain} = \frac{2.1(\text{kg / sec})}{(15-3)\text{psi}} = \frac{2.1}{12}(\text{kg / sec})/\text{psi}$$

The electropneumatic valve has a constant gain:

$$\frac{\Delta P}{\Delta I} = \frac{(15-3)\text{psi}}{(20-4)\text{mA}} = \frac{12}{16}\ (\text{psi/mA})$$

Including constant gain of current - to - pressure transducer in control - valve transfer function, $G_{(v)}(s)$, we get

$$G_{(v)}(s) = \frac{0.13}{3s+1} \qquad (21)$$

The sensor has calibrated range of 50° to 150°C and a 10sec time - constant.

$$\text{sensor gain} = \frac{16\ \text{mA}}{(150-50)℃} = 0.16\ (\text{mA/℃})$$

The transfer function of sensor has been given by:

$$H(s) = \frac{0.16}{10s+1} \qquad (22)$$

**Tuning of PID Controller**

On the basis of the transient response characteristics of a certain plant, Ziegler and Nichols provided guidelines for calculating the values of $K_P$, $K_I$, and $K_D$. Popular techniques for adjusting PID controllers include closed loop oscillations. A critical gain $K_C$ is induced in the control system's forward path using this type of tuning technique. The system is on the verge of instability that results from huge gain value. It causes oscillations, and the frequency and the time values are determined from oscillations. The experimental tuning guidelines in Table 1 are based on the closed loop oscillation technique [7, 8]

**Table 1:** Closed loop oscillation based tuning approaches.

| ***Controller Type*** | $K_p$ | $T_i$ | $T_d$ |
|---|---|---|---|
| *P* | $0.5K_c$ | 0 | 0 |
| *PI* | $0.45K_c$ | 0.83 T | 0 |
| *PID* | $0.6K_c$ | 0.5 T | 0.125 T |

*Tube side*

A crucial gain $K_c$ is induced in the control system's forward path using this type of tuning technique.

$$1 + G(s)H(s) = 0$$

$$1 + \left(\frac{0.13}{3s+1} * \frac{0.00052004177K_c}{19.99201771265s+1}\right) * \left(\frac{0.16}{10s+1}\right) = 0$$

$$599.7605313795s^3 + 289.89623026445s^2 + 32.99201771265s + 1 + 0.00001081687K_c = 0$$

$$\Longrightarrow \omega = 0.23453923111$$

$$\Longrightarrow K_c = 1381804.5827065608$$

$$T = \frac{2\pi}{\omega} \Longrightarrow T = 26.78948539843$$

$$K_P = 0.6K_c = 829082.7496239365$$

$$T_i = 0.5T = 13.39474269922$$

$$T_d = 0.125T = 3.3486856748$$

*Shell side*

$$1 + G(s)H(s) = 0$$

$$1 + \left(\frac{0.13}{3s+1} * \frac{0.0002557K_c}{10.2811487s+1}\right) * \left(\frac{0.16}{10s+1}\right) = 0$$

$$308.434461s^3 + 163.6549331s^2 + 23.2811487s + 1 + 0.00000531856K_c = 0$$

$$\Longrightarrow \omega = 0.27473927935$$

$$\Longrightarrow K_c = 2134590.5506026004$$

$$T = \frac{2\pi}{\omega} \Longrightarrow T = 22.86962869687$$

$$K_P = 0.6K_c = 1280754.3303615605$$

$$T_i = 0.5T = 11.43481434844$$

$$T_d = 0.125T = 2.85870358711$$

## Results and Discussion

This example data was taken from one of the previously published research, and these readings are applied in this research, and the results are presented and compared.

The transfer function of tube side is calculated from eq.(14).

$$G_1(s) = \frac{T_{c_o}(s)}{T_{h_o}(s)} = \frac{K_2}{\tau_1 s + 1}$$

$$K_2 = \frac{U_c A_c}{m_c c_{P_c} + U_c A_c} = \frac{317.4 * 0.048}{7.022 * 4200 + 317.4 * 0.048} = 0.00052$$

$$\tau_1 = \frac{\rho_c V_c c_{P_c}}{m_c c_{P_c} + U_c A_c} = \frac{986.4 * 0.145 * 4200}{.022 * 4200 + 317.4 * 0.048} = 19.992$$

The transfer function of shell side is calculated from eq.(20).

$$G_2(s) = \frac{T_{h_o}(s)}{T_{c_o}(s)} = \frac{K_4}{\tau_2 s + 1}$$

$$K_4 = \frac{U_h A_h}{m_h c_{P_h} + U_h A_h} = \frac{317.4 * 0.136}{37.012 * 4560 + 317.4 * 0.136} = 0.000256$$

$$\tau_2 = \frac{\rho_h V_h c_{P_h}}{m_h c_{P_h} + U_h A_h} = \frac{932.9 * 0.408 * 4560}{37.012 * 4560 + 317.4 * 0.136} = 10.281$$

**Table 2:** The transfer function of tube and shell side

| **The transfer function** | |
|---|---|
| **Tube side** | **Shell side** |
| $\mathbf{\frac{0.00052}{19.992\ S + 1}}$ | $\frac{0.000256}{10.281\ S + 1}$ |

After calculating these values, they are applied in MATLAB in order to know the response of each system and how it is controlled to obtain the best required state.

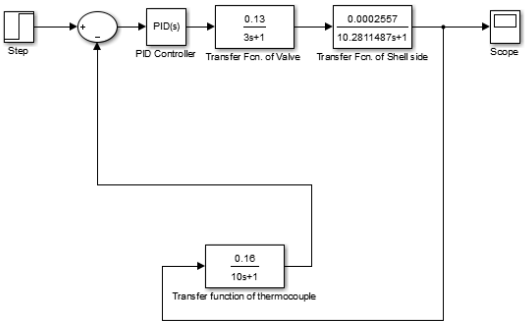


**Fig. 2** *The block diagram of tube side.*

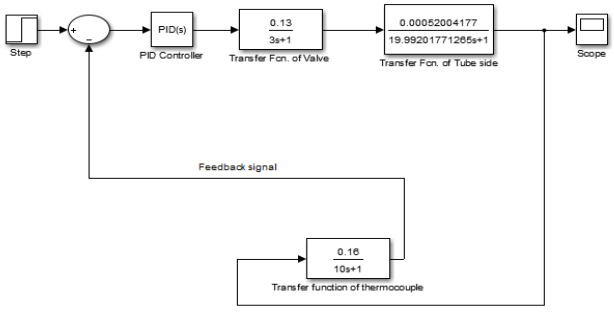


**Fig. 3** *The block diagram of shell side*

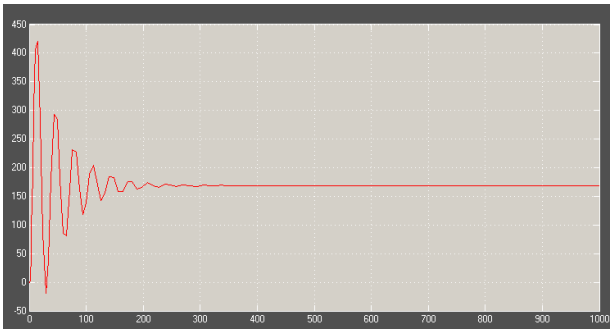


**Fig.4** *Response of P controller of tube*

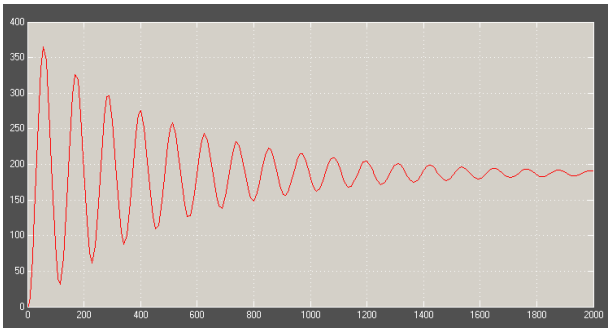


**Fig. 5** *Response of I controller of tube.*

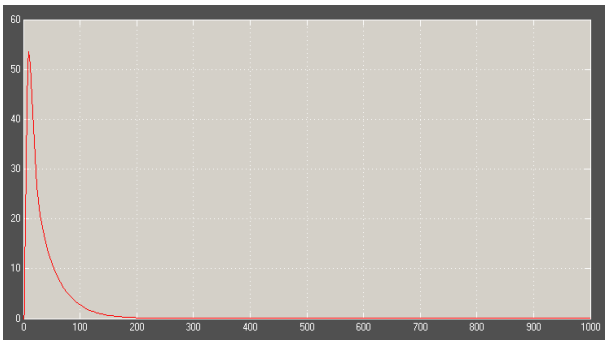


**Fig. 6** *Response of D controller of tube.*

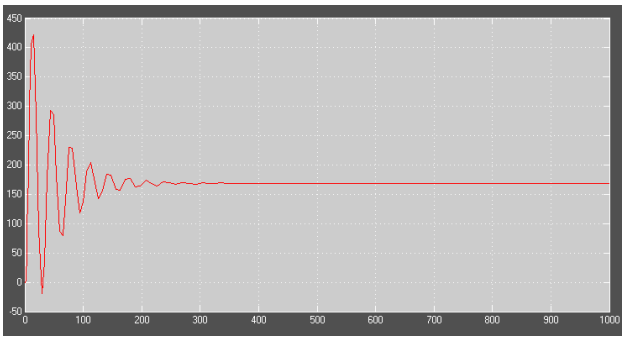


**Fig. 7** *Response of PI controller of tube.*

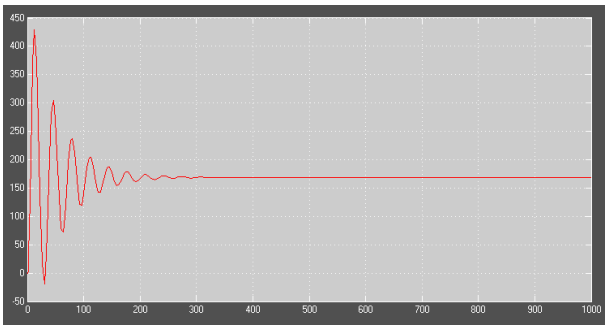


**Fig. 9** *Response of PD controller of tube.*

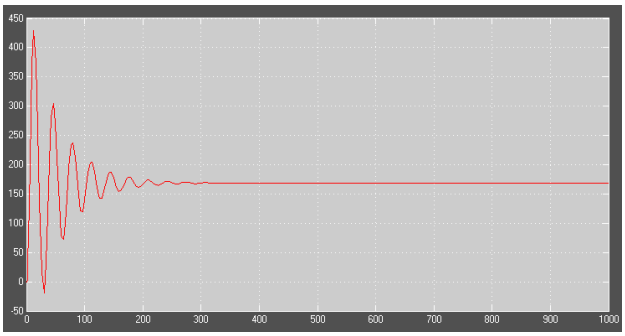


**Fig. 10** *Response of PID controller of tube.*

One of the key factors in the existence of disturbances in the heat exchanger process is the feed flow rate. The outlet temperature of the tube side effect decreases as the feed flow rate increases. Temperature variation in P controller occurs with a more delay time with respect to that of PID effect, but the temperature decrease is less than PID effect. The time constant of (P, I, D, PI and PD) are larger than the PID controller.

The outlet temperature of the tube side is lowered by increasing the flow rate, as indicated in Fig. 4 to Fig. 10. It may be seen from temperature responses that PID controllers arrive at a new steady-state condition more slowly than other controllers do. It was discovered during the discussion of the transfer function parameter that the time constant increases as the flow rate decreases.

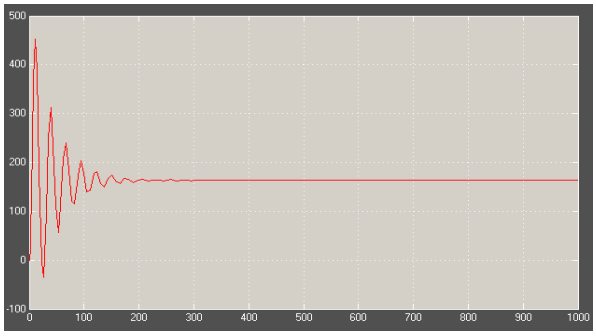


**Fig. 11** *Response of P controller of shell.*

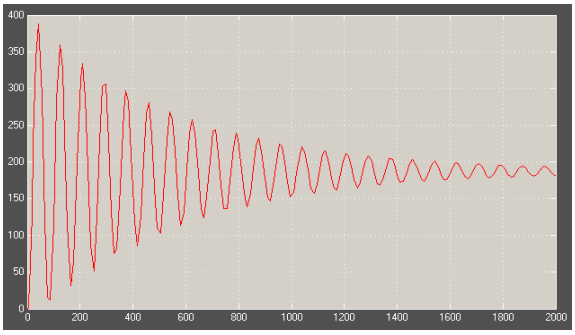


**Fig. 12** *Response of I controller of shell.*

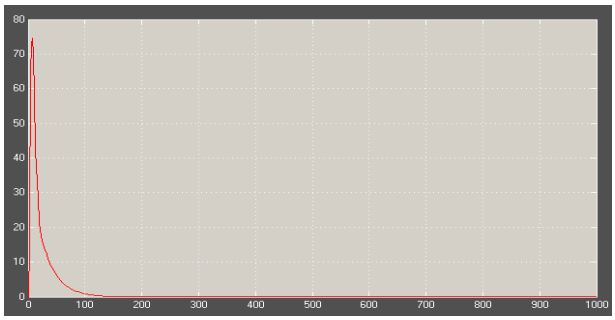


**Fig. 13** *Response of D controller of shell.*

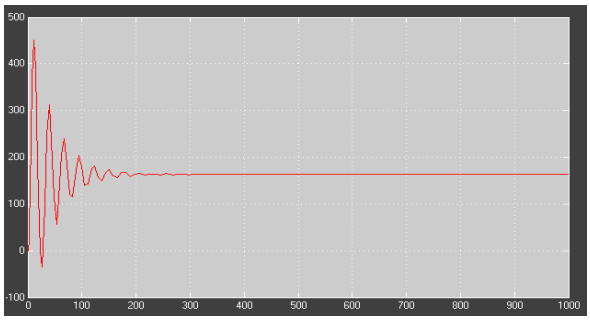


**Fig.14** *Response of PI controller of shell.*

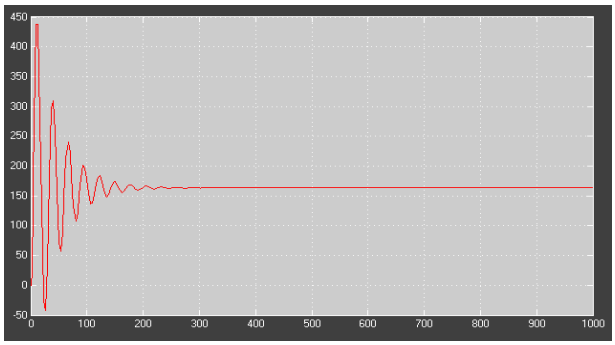


**Fig. 15** *Response of PD controller of shell.*

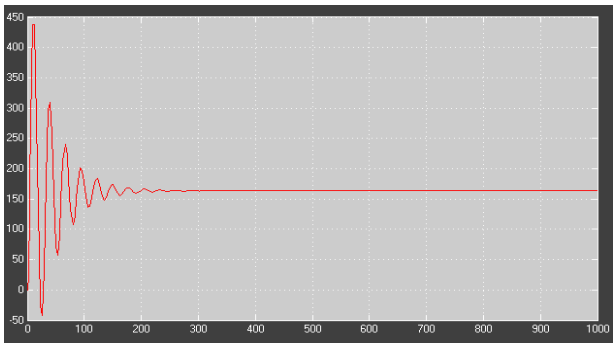


**Fig. 16** *Response of PID controller of shell.*

Fig. 11 to Fig. 16 demonstrate how the temperature sensitivity of the tube side increases as the steam flow rate increases. This is because higher steam flow rates result in more heating. Compared to PID controllers, responses from controllers (P, I, D, PI, and PD) lag more in time. It was discovered during the discussion of the transfer function parameter that the time constant decreased as the steam flow rate rose. Through increasing the steam flow rate, heat exchanger exit temperatures are raised. It can be seen from temperature response curves that impacts take longer to reach a new steady state condition. This is due to the fact that a heat exchanger needed a delay period to account for changes in inlet temperature. PID has a smaller time constant compared to other controllers.

**Table 4:** Comparison between the types of controllers with regard to overshoot and settling time of tube.

| Types of Controllers | Overshoot | Settling Time (Sec) |
|---|---|---|
| **P** | 149.4681 | 208.7294 |
| **I** | 0 | 980.6300 |
| **D** | $8.8638 \times 10^{6}$ | 90.6485 |
| **PI** | 150.0167 | 208.0441 |

| | | |
|---|---|---|
| **PD** | 154.3457 | 209.7858 |
| **PID** | 141.3435 | 194.7810 |

**Table 5:** Comparison between the types of controllers with regard to overshoot and settling time of shell.

| Types of Controllers | Overshoot | Settling Time (Sec) |
|---|---|---|
| **P** | 176.2222 | 165.9198 |
| **I** | 0 | 980.3313 |
| **D** | $7.8956 \times 10^6$ | 51.4494 |
| **PI** | 176.0551 | 165.8639 |
| **PD** | 167.7357 | 166.5375 |
| **PID** | 154.7334 | 158.5384 |

## Conclusion

Through Table 4 and Table 5, which show the types of controllers for each system, the best control system will be determined, which is the system that has the least possible overshoot and settling time. Various types of control systems have been used to determine the optimal sort of control system. By comparing the PID type control system to other control systems about both settling time and bypass or overshoot, the results showed that it is the best control system. So, the best type of controller for both systems is PID controller.

## References


[1] Zhang, L., Zhou, L., Ren, L., & Laili, Y. (2019). Modeling and simulation in intelligent manufacturing. Computers in Industry, *112*(103123). https://doi.org/10.1016/j.compind.2019.08.004

[2] Maghsoudali, Y., Rastegarkoutenaei, A., Sahami, M., & Bandpy, M. G. (2022). Investigation of the effect of using the finned tubes on the performance of shell and tube heat exchanger by 3D modeling. Journal of Energy Storage, *56* (106031). https://doi.org/10.1016/j.est.2022.106031

[3] Ilaiah, P. P. P. V. S., & Reddy, G. P. (2023). Real-Time Temperature Control of a Shell and Tube Heat Exchanger by IMC based PID controller. Proceedings of 38th International Confer,(vol. 91, pp. 155-163).

[4] Srivastava, N., Tanti, D. K., & Ahmad, M. A. (2014). Matlab simulation of temperature control of heat exchanger using different controllers. Autom. Control Intell. Syst, *2* (1), 1-5. https://doi.org/10.11648/j.acis.20140201.11

[5] Sarabeevi, G. M., & Beebi, M. L. (2016, September). Temperature control of shell and tube heat exchanger system using internal model controllers. In 2016 International Conference on Next Generation Intelligent Systems (ICNGIS) (pp. 1-6). IEEE.

[6] Ahmed, D. F., & Khalaf, Z. A. (2020, November). Intelligent controllers of multiple effect evaporators via simulation. In IOP Conference Series: Materials Science and Engineering (Vol. 928, No. 2, p. 022008). IOP Publishing.

[7] Chu, Y., Fei, J., & Hou, S. (2019). Adaptive global sliding-mode control for dynamic systems using double hidden layer recurrent neural network structure. IEEE transactions on neural networks and learning systems, *31*(4), 1297-1309. https://doi.org/10.1109/TNNLS.2019.2919676

[8] Liu, G., Su, Y., Zhu, W., Tian, M., Li, J., & Tian, Y. (2022). Numerical simulation of heat transfer in electrically heated footwear in a severely cold environment. Building and Environment, *207* (108429). https://doi.org/10.1016/j.buildenv.2021.108429

[9] Abbasi, H. R., Sedeh, E. S., Pourrahmani, H., & Mohammadi, M. H. (2020). Shape optimization of segmental porous baffles for enhanced thermo-hydraulic performance of shell-and-tube heat exchanger. Applied Thermal Engineering, *180* (115835). https://doi.org/10.1016/j.applthermaleng.2020.115835

[10] Guo, J., Du, Z., Liu, G., Yang, X., & Li, M. J. (2022). Compression effect of metal foam on melting phase change in a shell-and-tube unit. Applied Thermal Engineering, *206* (118124). https://doi.org/10.1016/j.applthermaleng.2022.118124

[11] Shojaeinasab, A., Charter, T., Jalayer, M., Khadivi, M., Ogunfowora, O., Raiyani, N., & Najjaran, H. (2022). Intelligent manufacturing execution systems: A systematic review. Journal of Manufacturing Systems, (vol. 62, pp. 503-522). https://doi.org/10.1016/j.jmsy.2022.01.004

[12] Sahoo, A., Radhakrishnan, T. K., & Rao, C. S. (2017). Modeling and control of a real time shell and tube heat exchanger. Resource-Efficient Technologies, *3*(1), 124-132. https://doi.org/10.1016/j.reffit.2016.12.001